# Archaeometric Investigations on Fragments of a Roman Statue Discovered at Porolissum

Mihai Munteanu, Ionel Chicinaş,
Coriolan Horaţiu Opreanu

## Introduction

In late 2013, during the archaeological excavations performed in the "custom" of the Roman camp of Porolissum (Moigrad, Sălaj County, Romania), a number of small metallic debris were discovered, grouped in the same area; among these, a consistent fragment of significant size (the fist of a hand, belonging to a colossal Roman statue) was identified (see Fig. 1).

Fig. 1. Fragment of a colossal Roman statue (the fist of a hand), discovered at Porolissum (two different views)

From the consistent fragment (the fist of a hand), a small sample was collected (*Mi1*) and from the group of all small metal pieces, only one sample was chosen (*Mi2*).

The purpose of this scientific endeavor was to investigate the possible common origin of the two fragments (*Mi1* and *Mi2*), which may have belonged to the same Roman imperial statue.

As a first stage of investigation, the two samples (*Mi1* and *Mi2*) were subjected to X-ray diffraction measurements. This method allows identifying the structure of the inves-

Fig. 2. The analyzed samples (*Mi1* and *Mi2*); we notice their small dimensions (*Mi1* has been collected from the consistent fragment—the fist of the hand—presented in Fig. 1)

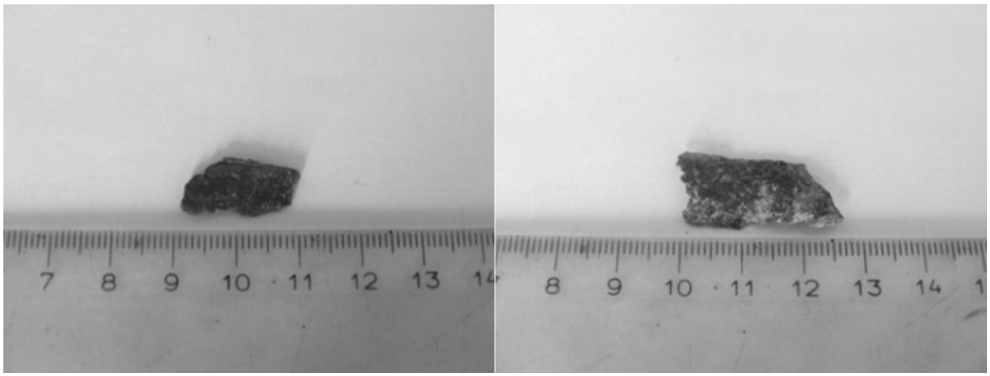


tigated crystalline systems, the determination of network constants and—by applying Fourier analysis to the diffraction peaks—to determine (by Rietveld analysis) the microstructure parameters and the substitution processes occurring during the replacement of the structure of the host material (by Rietveld analysis)[1] (Rietveld 1969; Klug and Alexander 1974; Altomare et al. 2001). The obtained results, previously published and discussed in Munteanu et al. 2014, are presented in Fig. 3:

Fig. 3. The X-ray diffractograms (X-ray diffraction patterns) for the two samples *Mi1* and *Mi2* contain the following crystalline compounds: ferrosilite ($FeSiO_3$—▽); copper (Cu—⊗) ; silicon dioxide (silica) ($SiO_2$—○); iron oxide ($Fe_3O_4$—♦ ) and amorphous component

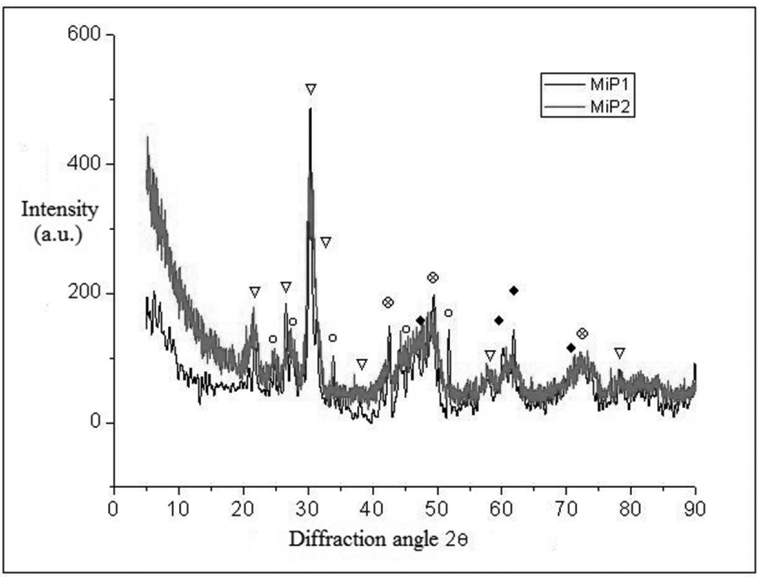

According to Figure 3, the investigated samples are multiphase systems, poorly crystallized, containing the crystalline compounds: ferrosilite ($FeSiO_3$—orthorhombic structure, Datasheet PDF 72-1509) (Sueno, Cameron, and Prewitt 1976; Martin 2004); copper (Cu—cubic structure, Datasheet PDF 04–0836) (Suh, Ohta, and Waseda 1988; Downs and Wallace 2003); silicon dioxide (silica) ($SiO_2$—tetragonal structure, Datasheet PDF 89-3606 ) (Downs and Wallace 2003) ; iron oxide ($Fe_3O_4$—spinel cubic structure, Datasheet PDF 19-0629) (Pluth, Smith, and Faber 1985). The analysis indicates that a significant fraction of these samples is amorphous, without a determined crystalline structure.

It was also noticed that the *Mi1* sample contains significantly higher amounts of ferrosilite ($FeSiO_3$) and copper (Cu) than *Mi2*, which could indicate that this sample comes from an area less exposed to corrosion. Then, the deformations of the crystalline network for the crystalline components of ferrosilite ($FeSiO_3$) and copper (Cu) in *Mi2* are significantly higher than in *Mi1*, which also indicates that this sample (*Mi2*) has undergone a more intense process of physical and chemical degradation (*Mi2*, being a small fragment detached from the body of the statue, suffered a more pronounced degradation comparing to *Mi1*) (Munteanu et al. 2014).

Based on these results, the possibility of the two samples (*Mi1* and *Mi2*) belonging to the same antique statue can be intuited (Munteanu et al. 2014), but only a quantitative determination of each chemical element found in the composition of the two fragments can bring additional evidence on this matter.

## Elemental Analysis and Results

AFTER FORMULATING some preliminary conclusions (by using the RX diffraction method) regarding the possible common origin of the samples *Mi1* and *Mi2* in the same statue, the only way to validate these results is to perform some measurements with the SEM microscope.

For this purpose, for each sample two distinctive areas were chosen, which were scanned at various resolutions (100x and 1000x), finally yielding the elemental composition and the planar distribution of the identified chemical elements.

**Analysis of the *Mi1* sample**

***a)100x resolution measurement***

A first measurement was carried out on an area of the sample, which was magnified 100 times (100x). The identified elements are presented in Fig. 4.

The chemical composition of the analyzed area (mass and atomic percentage) is presented in Table 1.

Fig. 4. The image of the analyzed area—*Mi1* sample (a). Identified elements, 100x resolution (b)

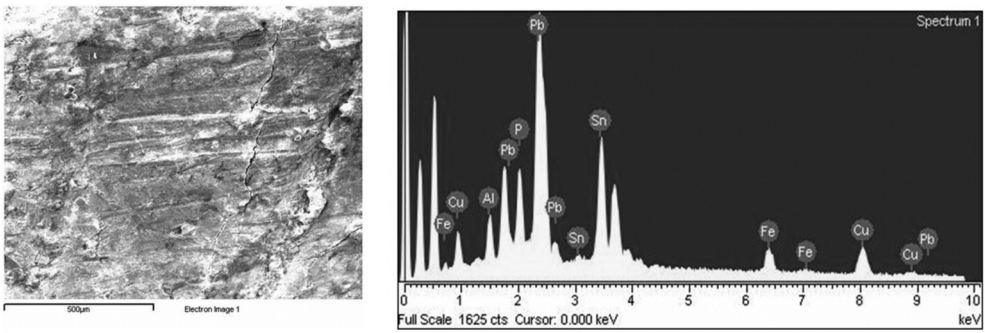


A B

Table 1. The identified chemical composition for the *Mi1* sample (100x resolution)

| Element | App. Conc. | Intensity Corrn. | Weight % | Weight % Sigma | Atomic % |
|---|---|---|---|---|---|
| Al K | 3.04 | 0.6361 | 3.77 | 0.12 | 13.47 |
| P K | 8.81 | 1.2573 | 5.53 | 0.13 | 17.21 |
| Fe K | 5.79 | 1.0136 | 4.51 | 0.24 | 7.78 |
| Cu K | 12.72 | 1.0588 | 9.48 | 0.41 | 14.38 |
| Sn L | 31.46 | 0.7507 | 33.07 | 0.43 | 26.85 |
| Pb M | 47.94 | 0.8666 | 43.65 | 0.48 | 20.31 |
| Totals | | | 100.00 | | |

***b)1000x resolution measurement***

A second measurement was performed by using a magnification factor of 1000x, on another area of the same sample *Mi1*. The identified elements are presented in Fig. 5, together with the chemical composition of the analyzed area (mass and atomic percent).

Fig. 5. The identified elements, 1000x resolution, on another area of *Mi1* sample

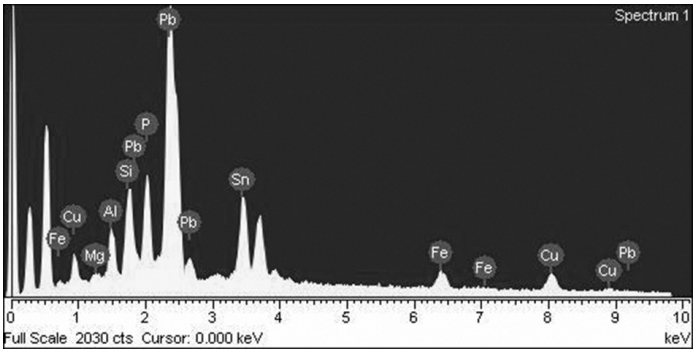

The chemical composition of the analyzed area (mass and atomic percentage) is presented in Table 2:

TABLE 2. THE IDENTIFIED CHEMICAL COMPOSITION FOR THE *MI1* SAMPLE (1000X RESOLUTION)

| Element | App. Conc. | Intensity Corrn. | Weight % | Weight % Sigma | Atomic % |
|---|---|---|---|---|---|
| Mg K | 0.40 | 0.5668 | 0.49 | 0.12 | 1.81 |
| Al K | 3.19 | 0.6879 | 3.27 | 0.12 | 10.84 |
| Si K | 6.05 | 0.8077 | 5.27 | 0.14 | 16.81 |
| P K | 9.73 | 1.2621 | 5.43 | 0.14 | 15.70 |
| Fe K | 4.75 | 1.0096 | 3.31 | 0.24 | 5.31 |
| Cu K | 9.33 | 1.0574 | 6.21 | 0.39 | 8.76 |
| Sn L | 24.90 | 0.7149 | 24.52 | 0.43 | 18.50 |
| Pb M | 62.99 | 0.8610 | 51.50 | 0.51 | 22.27 |
| TOTALS | | | 100.00 | | |

The resulted image of the analyzed area, together with the planar distribution of the identified elements, is presented in Fig. 6:

FIG. 6. THE IMAGE OF THE ANALYZED AREA (*MI1* SAMPLE, 1000X MAGNIFICATION FACTOR) (A). PLANAR DISTRIBUTION MAPS FOR PB (B), SI (C), P (D), FE (E), AL (F), CU (G) AND SN (H)

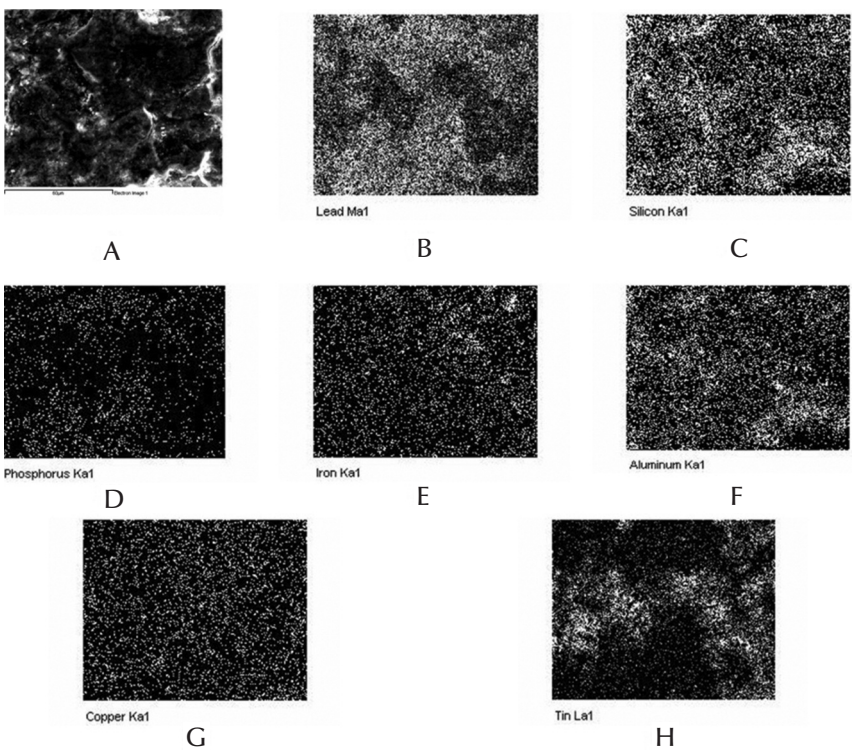

**Analysis of the *Mi2* sample**

***a)100x resolution measurement***

As in the case of the *Mi1* sample, a first measurement on sample *Mi2* was performed on an area that was magnified 100 times (100x magnification factor). The identified elements are presented in Fig. 7:

Fig. 7. The image of the analyzed area—*Mi2* sample (a). Identified elements, 100x resolution (b)

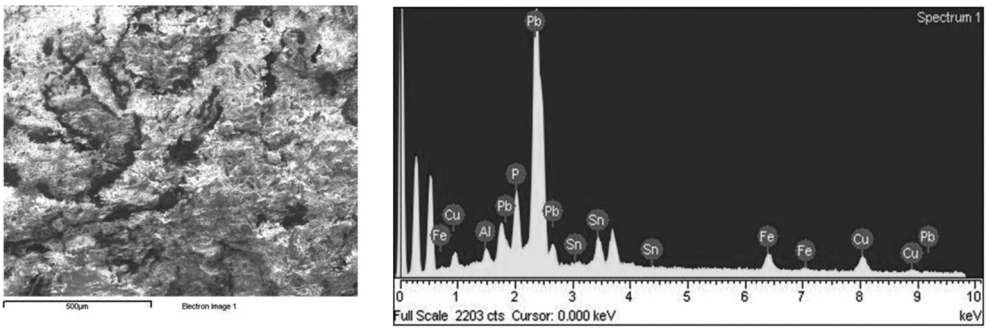


A B

The chemical composition of the analyzed area (mass and atomic percentage) is presented in Table 3:

Table 3. The identified chemical composition for the *Mi2* sample (100x resolution)

| Element | App. Conc. | Intensity Corrn. | Weight % | Weight % Sigma | Atomic % |
|---|---|---|---|---|---|
| Al K | 1.39 | 0.6905 | 1.77 | 0.10 | 7.38 |
| P K | 8.86 | 1.3913 | 5.58 | 0.12 | 20.27 |
| Fe K | 5.60 | 1.0443 | 4.70 | 0.23 | 9.46 |
| Cu K | 9.67 | 1.0953 | 7.73 | 0.38 | 13.69 |
| Sn L | 10.86 | 0.6866 | 13.85 | 0.35 | 13.13 |
| Pb M | 69.23 | 0.9132 | 66.38 | 0.47 | 36.06 |
| Totals | | | 100.00 | | |

***b)1000x resolution measurement***

In order to respect the symmetry of the measurements performed on the *Mi1* sample, an area of the *Mi2* sample was subjected to the same analysis, using a magnification factor of 1000 (1000x resolution). The identified elements are presented in Figure 8, together with the chemical composition of the analyzed area (mass and atomic percentage, in Table 4).

FIG. 8. THE IDENTIFIED ELEMENTS, 1000X RESOLUTION, ON ANOTHER AREA OF THE *MI2* SAMPLE

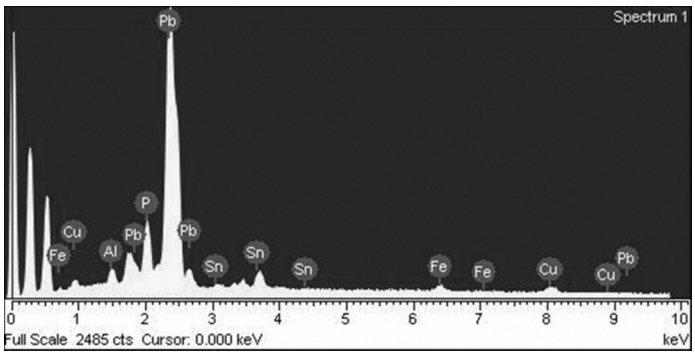


TABLE 4. THE IDENTIFIED CHEMICAL COMPOSITION FOR THE *MI2* SAMPLE (1000X RESOLUTION)

| Element | App. Conc. | Intensity Corrn. | Weight % | Weight % Sigma | Atomic % |
|---|---|---|---|---|---|
| Al K | 1.60 | 0.7545 | 2.15 | 0.09 | 10.20 |
| P K | 8.03 | 1.5010 | 5.42 | 0.11 | 22.35 |
| Fe K | 2.07 | 1.0592 | 1.98 | 0.20 | 4.53 |
| Cu K | 3.76 | 1.1262 | 3.38 | 0.33 | 6.80 |
| Sn L | 3.34 | 0.6509 | 5.19 | 0.31 | 5.59 |
| Pb M | 76.99 | 0.9524 | 81.88 | 0.45 | 50.52 |
| TOTALS | | | 100.00 | | |

Fig. 9 presents the resulted image of the analyzed area, together with the planar distribution of the identified elements.

The results of the EDX analyses obtained for the two samples *(Mi1* and *Mi2*) at the two considered resolutions (100x and 1000x) are comparatively presented in the following tables (the mass and atomic percentages were considered the most relevant information, and the elements Fe and Al were refined, as they did not play an important quantitative role in the alloy):

TABLE 5. COMPARISON BETWEEN *MI1* AND *MI2* (100X)

| 100x | *Mi1* | | *Mi2* | |
|---|---|---|---|---|
| | Weight % | Atomic % | Weight % | Atomic % |
| Pb | 43.65 | 20.31 | 66.38 | 36.06 |
| Sn | 33.07 | 26.85 | 13.85 | 13.13 |
| Cu | 9.48 | 14.38 | 7.73 | 13.69 |
| P | 5.53 | 17.21 | 5.58 | 20.27 |

Fig. 9. The image of the analyzed area (*Mi2* sample, 1000x magnification factor) (a); planar distribution maps for Pb (b), Si (c), P (d), Fe (e), Al (f), Cu (g) and Sn (h)

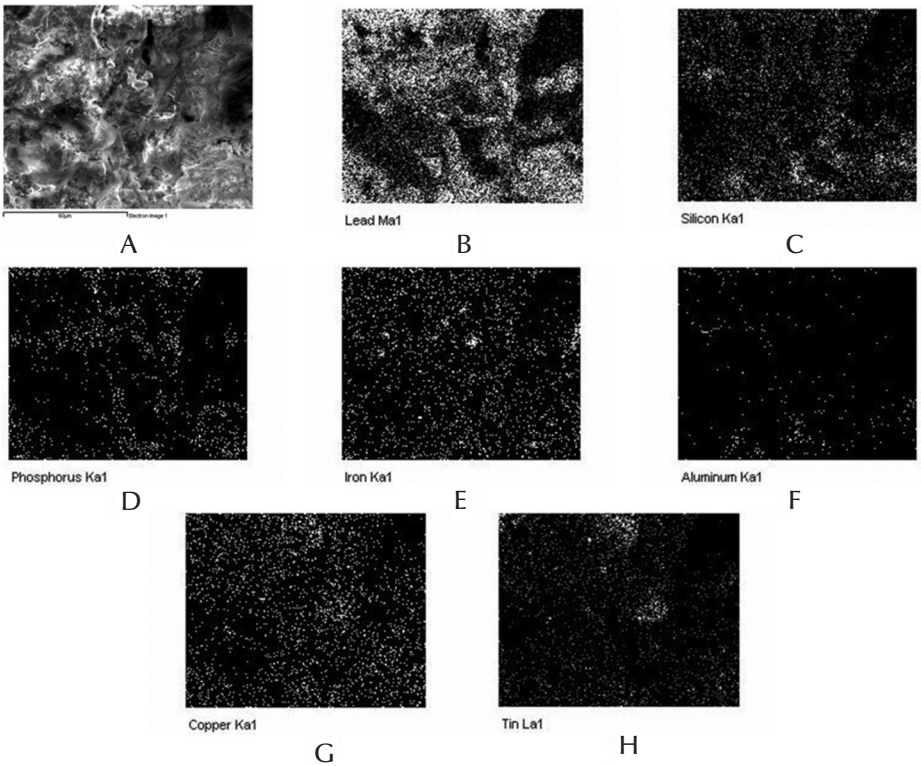


Table 6. Comparison between Mi1 and Mi2 (1000x)

| 1000x | *Mi1* | | *Mi2* | |
|---|---|---|---|---|
| | Weight % | Atomic % | Weight % | Atomic % |
| Pb | 51.50 | 22.27 | 81.88 | 50.52 |
| Sn | 24.52 | 18.50 | 5.19 | 5.59 |
| Cu | 6.21 | 8.76 | 3.38 | 6.80 |
| P | 5.43 | 15.70 | 5.42 | 22.35 |

The presence in the alloy of Copper (Cu) along with Tin (Sn) and Lead (Pb) should not be an anomaly at least for nowadays, given the fact that there are different bronzes known to contain these two metals in different proportions: "tin bronze," "leaded tin bronze" and "high leaded tin bronze" (Advance Bronze Incorporated). The problem with the analysis of these artifacts is that instead of a high percentage of Copper (Cu) (between 70 and 90%), the main metal in the alloy is Lead (Pb), followed by Tin (Sn) and only then Copper (Cu) (see Tables 5 and 6). Also, the presence of Phosphorus (P) in com-

bination with Copper (Cu) is known—even nowadays—in the so-called phosphorous bronzes, which contain—besides the high percentage of copper—an addition of phosphorus.

Then, it should be noted that in the *Mi2* sample, the percentage of Tin (Sn) and Copper (Cu) decreases compared to *Mi1*, while the percentage of Lead (Pb) increases. This can be explained by the fact that the *Mi2* sample, being smaller than *Mi1* (which was taken from the massive fist fragment of the statue), was subjected more aggressively to corrosion. Consequently, Copper (Cu) and Tin (Sn) "have disappeared" (they corroded quickly), leaving the heavy metal, Lead (Pb).

## Establishing the Height of the Statue

A LAST ISSUE related to this archaeometric investigation is the approximation of the initial height of the statue, based on the dimensions of its confirmed segments. Because the only part of consistent size that survived the passage of time is the fist, our approach has as starting point some measurements on this anatomical area.

FIG. 10. THE STATUE'S FIST DIMENSIONS

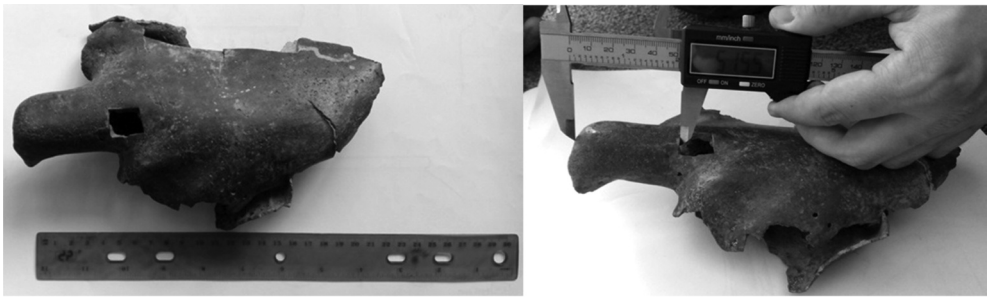

As can be observed from Fig. 10, the fist of the statue appears in a tight position, as if was holding something in the palm, with the middle finger bent after the first phalanx. Due to the fact that this anatomical part (the fist) is also fragmented (we cannot know precisely the delimitation between the palm and the forearm), the only segment fully preserved and which consequently can be used as a reference is the first phalanx of the middle finger. Thus, our approach aims to determine the height of the statue starting from the size of the first phalanx of the middle finger.

In 1973, the reputed surgeon J. William Littler proposed to the academic world the theory according to which the length of the phalanges is closely related to Fibonacci's sequence (Littler 1973). Recent studies have shown that the hypothesis is perfectly true for the little finger; in contrast, for the index, middle and the annular fingers, the dimensions of the phalanges are given by a mathematical relationship close to the sequence of Fibonacci, named Littler series, in honor of the distinguished surgeon (A. L. Hutchison and R. L. Hutchison 2010). As with the summative sequences, as the number of terms

tends to infinity, the ratio between a term in the sequence and the previous one will tend towards the number φ = 1,618, which represents the "golden proportion" (or the "golden number"), known from Antiquity. In metric terms, if there are two successive segments of different dimensions, the "golden proportion" refers to the ratio between the longest and the shortest segment.

Having two successive bone segments *a* and *b* (the phalanges of a finger in our case), according to the theory outlined above:

$$\frac{b}{a} = \frac{a+b}{b} = 1{,}6180 \ (1)$$

The middle finger has three phalanges: proximal, median, and distal, the size of which decreases successively, from the proximal to the other two.

Then, according to the relationship (1), starting from the known size of the proximal phalanx (according to the measurements presented in Fig. 10 is $p = 5{,}5\ cm$ long), the lengths of the other two phalanges and implicitly the length of the middle finger of the statue can be calculated.

Based on the performed calculations, the median phalanx has a length $m = 3{,}4\ cm$ and the distal $d = 2{,}1\ cm$, which means that the middle finger length $l_d$ is given by:

$$l_d = p + m + d = 5{,}5 + 3{,}4 + 2{,}1 = 11\ cm \ (2)$$

If we assume that the length of the palm of the statue (according to the measurements presented in Fig. 10) is $l_p = 11\ cm$ (and indeed, in anatomy it is known that the length of the middle finger is approximately the same as that of the palm), then the length of the segment from the wrist to the tip of the middle finger is:

$$l_t = l_d + l_p = 11 + 11 = 22\ cm \ (3)$$

***The first method for calculating the height of the statue***

According to Pretty Hands blog, there is a mathematical relationship (for male subjects) between the distance (in inches) from the wrist to the tip of the middle finger ($l_t$) and the height of a subject ($H$):

$$Hx0{,}11 = l_t \ (4)$$

That is, by multiplying the height $H$ of the subject (in inches) with a constant $k = 0.11$, the length of the distance between the wrist and the tip of the middle finger $l_t$ (still in inches) is obtained.

Based on these relationships, the height of the statue was estimated at about 2 m (the calculated value being $H = 199.94\ cm$).

***The second method for calculating the height of the statue***

Goncharova and Samokhoskaia (2011) propose a method of calculating the height of a human subject, by using different hand parameters (palm and finger bones), obtained using the X-ray imaging technique. But because this algorithm involves knowing the lengths of some bone segments which in the present case are impossible to determine (the fist is rather destroyed and twisted), this method was discarded.

Consequently, the second option to determine the height of the statue had as its starting point another study that highlighted the relationships between the different segments and parts of the human body (Kolodovski 2014).

Thus, according to this scientific approach, estimating the height of the studied statute is based on the following relationships (calculated for adult subjects older than 25):

- the length of the hand (from the palm wrist to the tip of the middle finger) is 1/4 of the length of the upper limb;
- the length of the upper limb is 3.5 times the height of the head;
- the height of the body is 8 times the height of the head.

Taking into account these relationships, the height of the statue was estimated at about 2.01 m (the calculated value being $H = 201.12$ *cm*).

The fact that both methods provided the same result (the difference between the two estimates is only 0.5%) points out that these calculations are relevant and that indeed, the original size of the statue was about 2 meters.

## Conclusions

THE PAPER discusses the archaeometric investigations carried out on two artifacts discovered in the ancient customs house of Porolissum: a metal fist of an imperial-age statue and a metallic splinter randomly selected from a multitude of small size fragments, found in the same area as the fragment of considerable size (the fist).

Thus, a first purpose of the research was to identify the possibility of the two fragments belonging to the same statue.

The starting point of this endeavor is a previous study, conducted by the same team, which focused on the X-ray diffraction analysis of the samples and which presumed the provenance of fragments from the same statue. In order to provide a verdict of high accuracy, the research continued with EDX elemental analyses, made for each sample in two different points and at different resolutions (100x and 1000x); in this way, the proportion of chemical elements in each sample was identified, on the basis of which it was concluded that the two fragments come from the same statue.

Finally, the proposed archaeometric investigation also aimed at determining the height of the statue, based on mathematical algorithms, which had to take into account the only intact segment of the statue, the proximal phalanx of the middle finger. Thus, the size of the statue was calculated by two different methods, but which provided the same result—a height of about 2 meters.

❑

## Note

1. The International Center for Diffraction Data (ICDD)—PDF-2 Release 2012—contains 250,182 data entries from the ICDD experimental powder data collection, as well as data collected, edited and standardized from ICSD databases. http://www.icdd.com/products/pdf2.htm.

## References

Advance Bronze Incorporated. http://www.advancebronze.com.

Altomare, A., M. C. Burla, C. Giacovazzo, A. Guagliardi, A. G. G. Moliterni, G. Polidori, and R. Rizzi. 2001. Quanto: a Rietveld program for quantitative phase analysis of polycrystalline mixtures. *Journal for Applied Crystallography* 34, 3: 392–397.

Downs, R. T. and M. Hall-Wallace. 2003. The American Mineralogist Crystal Structure Database. *American Mineralogist* 88, 1: 247–250.

Goncharova, N. N. and O. V. Samokhodskaia. 2011. Determination of the body length of an adult subject from the measurable wrist parameters on an X-ray image. [In Russian]. *Sudebno-meditsinskaya ekspertiza* 54, 4: 19–22.

https://prettyhands.wordpress.com/big-hands-for-your-height-a-way-to-find-out.

Hutchison, A. L. and R. L. Hutchison. 2010. Fibonacci, Littler, and the Hand: A Brief Review. *Hand* 5, 4: 364–368.

Klug, H. P. and L. E. Alexander. 1974. *X-ray Diffraction Procedures for Polycrystalline and Amorphous Materials*. 2nd edition. New York–Sydney–Toronto: John Wiley & Sons.

Kolodovski, I. I. 2014. Proportions of the human body. [In Russian]. Vitebsk: P. M. Masherov State University.

Littler, J. W. 1973. On the adaptability of man's hand (with reference to the equiangular curve). *Journal of Hand Surgery* 5, 3: 187–191.

Martin, J. D. 2004. Using XPowder: A software package for Powder X-Ray diffraction analysis. D.L. GR 1001/04. www.xpowder.com.

Munteanu, M., E. Indrea, C. Opreanu, and R. Ciorap. 2014. Micro-structural investigation of some artifacts discovered at Porolissum. *JIDEG: Journal of Industrial Design and Engineering Graphics* 9. Special Issue: Papers of the International Conference on History and Technology at the Black Sea Region, ISTM 2014, Ovidius University of Constanţa, Romania, 12–13 September 2014: 135–138.

Pluth, J. J., J. V. Smith, and J. Faber. 1985. Crystal structure of low cristabalite at 10, 293 and 473 K: Variation of framework geometry with temperature. *Journal of Applied Physics* 57, 4: 1045–1049.

Rietveld, H. M. 1969. A Profile Refinement Method for Nuclear and Magnetic Structures. *Journal for Applied Crystallography* 2, 2: 65–71.

Sueno, S., M. Cameron, and C. T. Prewitt. 1976. Orthoferrosilite: High-temperature crystal chemistry. *American Mineralogist* 61, 1–2: 38–53.

Suh, I.-K., H. Ohta, and Y. Waseda. 1988. High-temperature thermal expansion of six metallic elements measured by dilatation method and X-ray diffraction. *Journal of Materials Science* 23, 2: 757–760.

**Abstract**

Archaeometric Investigations on Fragments of a Roman Statue Discovered at Porolissum

The paper presents the investigation of two fragments of roman bronze artifacts, discovered during archaeological works performed at Porolissum, an important military and economic center on the northern limes of Dacia Province. One of the analyzed fragments (*Mi1*) was taken from a consistent fragment of a Roman statue, while the second (*Mi2*) was among a lot of small metal pieces, discovered in the same investigated area. Using highly sophisticated micro-structural analysis techniques (X-Ray diffraction, SEM-EDX) the paper investigates the possibility of *Mi1* and *Mi2* belonging both to the same roman statue. Also, based on the dimensions of the hand and fingers, the height of the statue was approximated.

**Keywords**

fragments of Roman statue, RX analysis, SEM-EDX analysis, establishing the height of the statue